Tweek, an Evolutionarily Conserved Protein, Is Required for Synaptic Vesicle Recycling

Patrik Verstreken,[1,4,5,7] Tomoko Ohyama,[1,7] Claire Haueter,[1] Ron L.P. Habets,[4,5] Yong Q. Lin,[1] Laura E. Swan,[6] Cindy V. Ly,[2] Koen J.T. Venken,[1,3] Pietro De Camilli,[6] and Hugo J. Bellen[1,2,3,*]
[1]Department of Molecular and Human Genetics and Howard Hughes Medical Institute
[2]Department of Neuroscience
[3]Program in Developmental Biology
Baylor College of Medicine, One Baylor Plaza, Houston, TX 77030, USA
[4]VIB, Department of Molecular and Developmental Genetics
[5]K.U.Leuven, Center for Human Genetics
Program in Molecular and Developmental Genetics, Program in Cognitive and Molecular Neuroscience, Laboratory of Neuronal Communication, Herestraat 49, B-3000 Leuven, Belgium
[6]Department of Cell Biology, Howard Hughes Medical Institute, Kavli Institute for Neuroscience, Yale University School of Medicine, New Haven, CT 06510, USA
[7]These authors contributed equally to this work
*Correspondence: hbellen@bcm.tmc.edu
DOI 10.1016/j.neuron.2009.06.017

SUMMARY

Synaptic vesicle endocytosis is critical for maintaining synaptic communication during intense stimulation. Here we describe Tweek, a conserved protein that is required for synaptic vesicle recycling. *tweek* mutants show reduced FM1-43 uptake, cannot maintain release during intense stimulation, and harbor larger than normal synaptic vesicles, implicating it in vesicle recycling at the synapse. Interestingly, the levels of a fluorescent $PI(4,5)P_2$ reporter are reduced at *tweek* mutant synapses, and the probe is aberrantly localized during stimulation. In addition, various endocytic adaptors known to bind $PI(4,5)P_2$ are mislocalized and the defects in FM1-43 dye uptake and adaptor localization are partially suppressed by removing one copy of the phosphoinositide phosphatase *synaptojanin*, suggesting a role for Tweek in maintaining proper phosphoinositide levels at synapses. Our data implicate Tweek in regulating synaptic vesicle recycling via an action mediated at least in part by the regulation of $PI(4,5)P_2$ levels or availability at the synapse.

INTRODUCTION

Synaptic vesicle recycling relies heavily on clathrin-dependent endocytosis, ensuring a continuous supply of new synaptic vesicles during stimulation (Haucke, 2003; Kasprowicz et al., 2008). Numerous proteins involved in the process have been identified through biochemical screening approaches and forward genetic screens in model organisms (Babcock et al., 2003; Jung and Haucke, 2007). Several protein adaptors and lipids coordinately bind and recruit downstream effectors that mediate membrane bending to shape new vesicles. The coordinated action of dynamin and its effectors results in separation of new vesicles that are subsequently prepared for a new round of fusion (van der Bliek and Meyerowitz, 1991). While numerous proteins and lipids have been assigned a specific function during this process, others play a supporting role to scaffold synaptic zones, ensuring a high fidelity of recycling (Koh et al., 2004; Majumdar et al., 2006).

Phosphoinositide lipids (PIs) play important regulatory roles in various cellular processes, including vesicle recycling (Martin, 1998; Vicinanza et al., 2008). $PI(4,5)P_2$ is concentrated at the plasma membrane of most cells, including neurons, and plays multiple roles in the regulation of synaptic transmission (Cremona et al., 1999; Di Paolo et al., 2004; Harris et al., 2000; Micheva et al., 2001; Van Epps et al., 2004; Verstreken et al., 2003). $PI(4,5)P_2$ is a precursor for the phospholipase C-derived metabolites, IP_3 and DAG, which are involved in the regulation of Ca^{2+} release from intracellular stores and vesicle priming and fusion, respectively (Davis and Patrick, 1990; Rhee et al., 2002; Sladeczek, 1987). $PI(4,5)P_2$ also appears to regulate the size of the readily releasable pool of synaptic vesicles and secretory granules (Di Paolo et al., 2004; Gong et al., 2005; Milosevic et al., 2005). In addition, $PI(4,5)P_2$ is implicated in the formation of new synaptic vesicles at the plasma membrane (Cremona et al., 1999; Harris et al., 2000; Mani et al., 2007; Van Epps et al., 2004; Verstreken et al., 2003). Hence, at the synapse, altered levels of $PI(4,5)P_2$ may affect several steps in the synaptic vesicle cycle. However, despite these pleiotropic functions, PI metabolism within the cell is surprisingly spatially restricted and PI-dependent processes appear to be locally regulated (Di Paolo et al., 2002; Golub and Caroni, 2005; Schuske et al., 2003).

Here we report the identification and characterization of a Tweek, a conserved and previously uncharacterized protein. Tweek is required to maintain normal synaptic vesicle recycling and affects PI availability. Our data suggest that Tweek may regulate synaptic vesicle recycling, at least in part, by affecting $PI(4,5)P_2$ pools at the synapse.
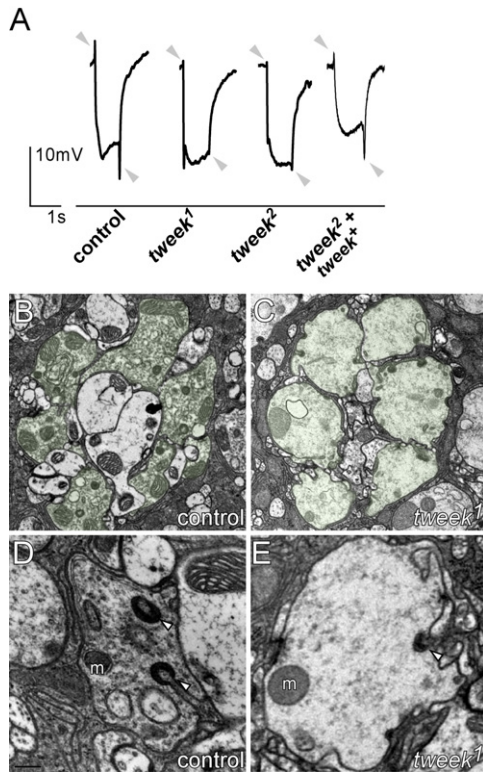
A

10mV

1s

control tweek[1] tweek[2] tweek[2] + tweek[+]

Figure 1. *tweek* **Mutant Photoreceptors Show Synaptic Defects**
(A) Electroretinograms of controls (*y w eyFLP; P{y[+] FRT40A/l(2)cl-2L P{w[+]} FRT40A*), *tweek* mutants (*y w eyFLP; tweek[1 or 2] P{y[+]} FRT40A/l(2)cl-2L P{w[+]} FRT40A*), and rescued *tweek* animals (*y w eyFLP; tweek[2] P{y[+]} FRT40A; tweek[+](HB69)/+*). The positions of "on" and "off" transients (or lack thereof) are indicated by gray arrows.
(B and C) Electron microscopy of control (*y w eyFLP; P{y[+]} FRT40A/l(2)cl-2L P{w[+]} FRT40A*) and *tweek[1]* mutant (*y w eyFLP; tweek[1] P{y[+]} FRT40A/l(2)cl-2L P{w[+]} FRT40A*) lamina cartridges. PR terminals of one cartridge are artificially labeled in green.
(D and E) Electron microscopy images of single PR terminals of control (C) and *tweek[1]* mutant (D) animals. Capitate projections (arrowhead) and mitochondria (m) are indicated.

RESULTS

Isolation of *tweek* Mutants

To identify proteins that affect synaptic transmission and plasticity, we performed genetic screens using *eyFLP* technology (Newsome et al., 2000; Stowers and Schwarz, 1999; Verstreken et al., 2003). These screens allow us to identify flies that carry random chemically induced (EMS) mutations that affect synaptic transmission in photoreceptors, circumventing the organismal lethality associated with these mutations. Flies with mutant eyes were screened by recording electroretinograms (ERGs) (Figure 1A). ERGs measure differences in extracellular potential between photoreceptors (PRs) and the body during a short light flash (1 s). In controls, ERG recordings show (1) a de- and repolarization of the PRs, reflecting an intact phototransduction mechanism and (2) "on" and "off" transients at the onset and conclusion of the light pulse, indicating that the PRs can activate postsynaptic neurons (Figure 1A, gray arrowheads). By isolating

mutants with defective on and off transients but normal depolarization, we and others have been able to identify genes that affect synaptic function or development (Babcock et al., 2003; Verstreken et al., 2003). Two mutations in one of the complementation groups on chromosome arm 2L, *tweek*, show "on" and "off" transient amplitudes that are severely reduced compared to controls (Figure 1A). These data suggest that *tweek* mutant PRs fail to properly transmit information to postsynaptic neurons.

To better understand the underlying cause of the defect in neuronal communication in *tweek* mutant eyes, we performed transmission electron microscopy (TEM), revealing ultrastructural features of the mutant PR synapses, including mitochondrial density and morphology, active zone integrity, glial cell morphology, and synaptic vesicle density. PRs invade the lamina, the first optic neuropil of the fly brain, cluster in groups of six, and form characteristic topographic connections on postsynaptic cells. One such unit, containing six PRs, labeled green in Figures 1B and 1C, is a lamina cartridge. Qualitative analyses indicate that most synaptic components are normal in *tweek* mutant PR terminals (Figures 1B–1E); however synaptic vesicle density appears markedly reduced (Figures 1D and 1E). In addition, although the numbers of glial invaginations in the PR cells (capitate projections) are not different between controls and mutants (controls: 0.355 ± 0.026 capitates μm^{-1}; *tweek[1]*: 0.352 ± 0.041 μm^{-1}; $p < 0.01$), capitate projections are not deeply invaginated or headed in the mutants but often remain shallow (controls: $17.9\% \pm 4.1\%$ shallow projections and *tweek[1]*: $68.3\% \pm 13.9\%$ shallow projections; $p < 0.01$; Figures 1D and 1E). Because glial invaginations are thought to be sites of endocytosis in PR terminals (Fabian-Fine et al., 2003), these data, together with the lower vesicle density, suggest that whereas development of the PR terminals is not much impaired, mutations in *tweek* may affect synaptic function, possibly endocytosis.

tweek mutants further sparked our interest as rare homozygous flies survive to adulthood. These flies are unable to walk or stand upright for long periods and exhibit seizures, suggestive of severe neurological defects. Based on the adult behavior of the mutants we named the gene "*tweek*" as it reminded us of the cartoon character "Tweek" from the TV series "South Park." However, even when grown under optimal conditions (see Experimental Procedures) most homozygous *tweek[2]* or transheterozygous *tweek[1]/Df* and *tweek[2]/Df* mutants die as late pupae, and only very few animals eclose (<1/2000) and die soon after eclosion. Hence, *tweek* is an essential gene.

tweek Encodes a Large Protein of Unknown Domain Structure

To identify the gene encoding *tweek*, we used meiotic recombination to map the lesions in the mutants (Zhai et al., 2003). Rough mapping placed *tweek* in the 36A–C cytological interval and showed that the mutations fail to complement *Df(2L)Exel8036* (Parks et al., 2004). Meiotic fine-mapping (Figure 2A) allowed us to map the lesions in the *tweek* alleles between *EY12630* and *KG05250*.

To confirm the mapping position we crossed the *tweek* EMS alleles to flies that carry lethal transposon insertions in the region. The *piggyBac* insertion *c01084* (Parks et al., 2004) located downstream of the start codon in *CG15133* as well as the *P* element
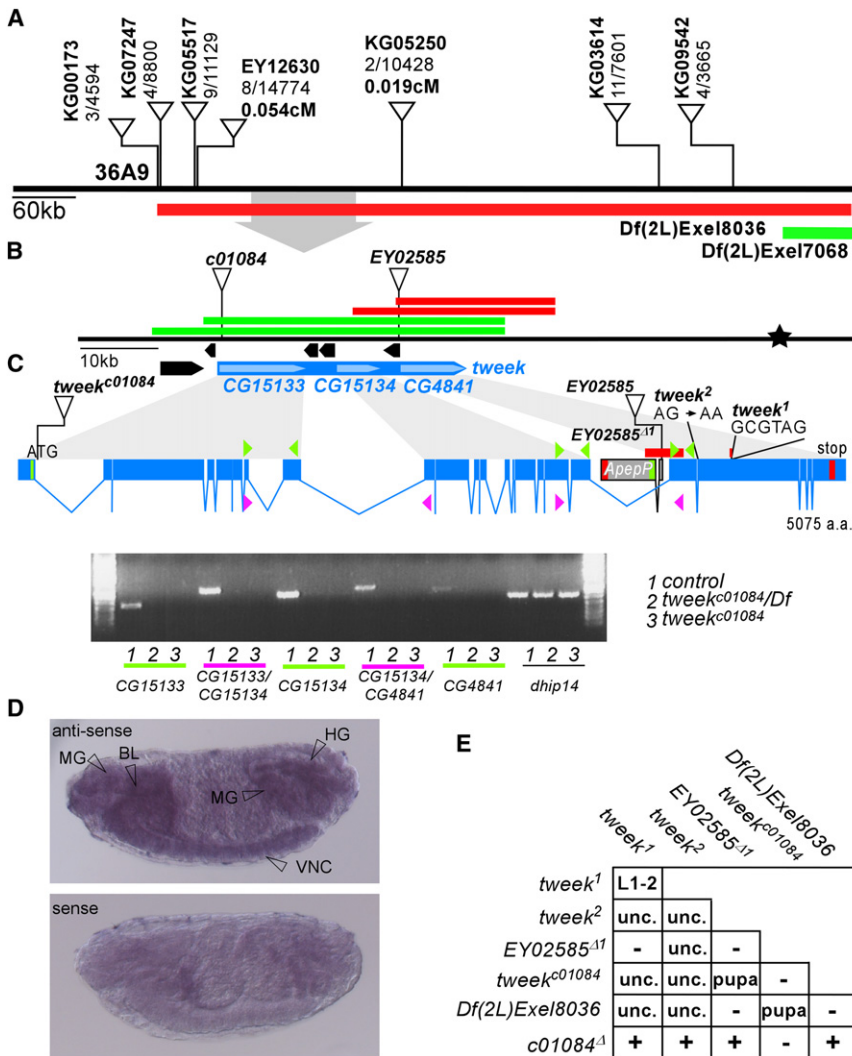
Figure 2. Characterization of *tweek* Mutants

(A) *P* element mapping. *P* elements used for mapping: numbers separated by a "/" indicate the number of recombinants out of flies scored. Recombination distance in cM for two nearby *P* elements is indicated. The cytological interval and the Exelixis deficiencies that complement (green) or not (red) are shown. The area magnified in (B) is shown by a gray arrow.

(B) The mapping location of *tweek* (blue) based on recombination data (star). *CG15133*, *CG15134*, and *CG4841* correspond to the *tweek* gene. *EY02528* as well as *c01084* fail to complement the *tweek*[1] and *tweek*[2] alleles. The regions cloned in P[acman] to create rescue constructs are indicated: red constructs do not rescue the *tweek* alleles whereas the green constructs do rescue the *tweek* alleles.

(C) Intron-exon structure of *tweek* and RT-PCR analysis. Start codons are marked in green and stop codons in red. The *P* element excision *EY02585*[Δ1] and the molecular nature of both *tweek* alleles are indicated. *tweek*[1] harbors a 74 bp deletion (red) and a 6 bp insertion (indicated) and *tweek*[2] harbors a splice acceptor mutation before exon 20. Agarose gel of RT-PCR on *y w eyFLP; FRT40A*[iso] control, *tweek*[c01084], and *tweek*[c01084]/*Df(2L)Exel8036* using the primers shown in Table S1.

(D) In situ hybridization of dioxygenin-labeled RNA to whole stage 15 embryos using a *CG4841* probe revealing labeling in the mid gut (MG), hind gut (HG), brain lobe (BL), and ventral nerve cord (VNC). An independent probe against *CG15134* shows an identical labeling pattern (see Figure S3) whereas sense probes do not show specific labeling.

(E) Lethal stage of *tweek* mutant combinations. L1-2: animals do not survive beyond the first or second instar larval stage. Pupa or unc: most animals die during the pharate adult (late pupal) stage. However, very few (<1/2000) manage to eclose but are severely uncoordinated. −: failure to complement, +: complement.

insertion *EY02585* (Bellen et al., 2004) located between *ApepP* and *CG4841* and an imprecise excision of this *P* element (*EY02585*[Δ1]), removing the start codons of *ApepP* and *CG4841*, all fail to complement the *tweek* alleles and *Df(2L)Exel8036* (Figures 2B, 2C, and 2E). An excision of the *piggyBac* insertion (*c01084*[Δ] in Figure 2E) and a precise excision of the *P* element revert the lethality and complement the *tweek* alleles and the deficiency. Although *CG15133* and *CG4841* are separated by four genes encompassing more than 12 kb, *c01084* and *EY02585*[Δ1] also fail to complement one another, suggesting that both mutations affect the same gene.

As shown in Figure 2B, *CG15134* is the only gene located between *CG15133* and *CG4841* that is transcribed in the same orientation. To determine if *CG15133*, *CG15134*, and *CG4841* encode a single gene, we performed RT-PCR experiments with cDNAs prepared from control, *c01084*[Δ], *c01084*/*Df*, and homozygous *c01084* flies. Although we were able to amplify and sequence control and *c01084*[Δ] cDNA fragments using primers in *CG15133* and *CG15134*, primers in *CG15134* and *CG4841*, and primers in *CG15133* and *CG4841* (Figure 2C, data not shown, and Table S1 available online), no such fragments could be recovered from homozygous *c01084* animals. Hence, our data indicate that *CG15133*, *CG15134*, and *CG4841* can form one transcript. Furthermore, the *piggyBac* (*c01084*) insertion in *CG15133* greatly reduces or abolishes expression of these three separately annotated *CG*s, suggesting that it is a strong hypomorphic or null allele of *tweek*. Hence, *CG15133*, *CG15134*, and *CG4841* are jointly transcribed as a large transcript and this transcript corresponds to *tweek*.

The 5′ untranslated region (UTR) of *tweek* is not annotated, and we therefore performed rapid amplification of 5′ complementary DNA ends (5′RACE). We were able to amplify 108 bp 5′ of the ATG start codon in *CG15133*, identifying the 5′UTR of *tweek*. These data also place the *c01084* insertion inside *tweek*, and we therefore renamed *c01084* as *tweek*[c01084]. However, the previously annotated second exon of *CG15133* does not appear

amplifiable in our assays, and the gene structure based on our RT-PCR and 5′RACE results is shown in Figure 2C.

We also found a 74 bp deletion and a 6 bp insertion leading to a premature stop codon in *tweek[1]* and an AG to AA splice acceptor mutation before exon 20 in *tweek[2]*, predicting a frame shift (Figure 2C). This splice acceptor mutation in *tweek[2]* was also confirmed by RT-PCR (Figure S1 and Table S1). Since *tweek[c01084]*/*tweek[1]*, *tweek[c01084]*/*tweek[2]*, *tweek[1]*/*Df(2L)Exel8036*, *tweek[2]*/*Df(2L)Exel8036*, *tweek[c01084]*/*Df(2L)Exel8036*, and *tweek[2]*/*tweek[2]* show a similar lethal phase, our data suggest that *tweek[c01084]*, *tweek[1]*, and *tweek[2]* are all severe hypomorphic alleles or null alleles of *tweek* (Figure 2E). Finally, *tweek* corresponds to *CG15133*, *CG15134*, and *CG4841* as all mutations in *trans* over a *Df* can be rescued using P[acman] clones (Venken et al., 2006) that contain genomic DNA encompassing *CG4841*, *CG15133*, and *CG15134* (Figure 1A, green bar in Figure 2B, and Table S2); however, the *tweek* alleles cannot be rescued with a 21 kb construct encompassing the *CG4841* sequence (red bar in Figure 2B). Based on sequence annotation and RT-PCR data, our data indicate that the *tweek* mRNA transcript is 16,124 bp and the Tweek protein encompasses an open reading frame (ORF) of 5076 amino acids (~565 kDa). Although *tweek* encodes a very large and evolutionarily conserved protein, it contains no known protein domains or motifs, including transmembrane domains or nuclear localization signals. Nonetheless, BLAST searches reveal that Tweek has homologs from nematode to man (Figure S2). In most species including various Drosophilids, mosquitoes, and mouse, the three CGs identified as *tweek* correspond to two or three adjacent transcripts annotated as two or three genes. In human, the *tweek* homolog is annotated as a single 138 kb gene encoding a very large protein named Fsa (Cao et al., 2006; Kuo et al., 2006). Although the predicted amino acid sequence of *Drosophila* Tweek aligns well with its human counterpart over the full-length protein (e.g., 30% identity with mouse Tweek), there are numerous regions that show much higher similarity and identity than the remaining areas (Figure S2). Hence, the sequence of Tweek does not reveal any particular information about its possible function.

To determine the expression pattern of *tweek* we performed in situ hybridization to embryos. As shown in Figure 2D, *tweek* is widely expressed but enriched in the brain lobes and in the ventral nerve cord after stage 14 of embryogenesis. We also observe expression in the midgut anlagen. Expression in the CNS becomes stronger in stage 15 embryos. These data are consistent with RT-PCR analyses that reveal expression of human Tweek/Fsa in the brain (McKay et al., 2003). Antisense dioxygenin-labeled RNA probes complementary to the two different *CGs* show identical RNA expression patterns (Figures 2D and S3). Moreover, the gene located 5′ of *CG15133* reveals a very different expression pattern than that of the *tweek* CGs (data not shown). Hence, *tweek* encodes a very large transcript that is expressed in the nervous system.

tweek Mutants Display Defects in Neurotransmitter Release upon Repetitive Stimulation

Drosophila mutations that affect synaptic vesicle exocytosis show reduced neurotransmitter release during low-frequency stimulation, (e.g., *SNAP25*, *syntaxin*, *CSP*, *hip14*, *cacoaphony*),

whereas mutations that affect endocytosis or recycling (e.g., *endophilin*, *AP180/lap*, *synaptojanin*, *eps15*, *dap160*, *synapsin*) do not affect release under such conditions. Hence to determine if *tweek* affects synaptic transmission, we first stimulated motorneurons at low frequency in the presence of 1 or 5 mM Ca^{2+} and recorded excitatory junctional potentials (EJPs). Neither the resting membrane potential nor the amplitude of the EJPs recorded during low-frequency stimulation (<1 Hz) in various *tweek* mutants are different from controls (Figures 3A, S4A, and S4B). These data indicate that *tweek* mutations do not dramatically impair exocytosis under these conditions.

Next we tested the ability of *tweek* mutants to maintain release during intense stimulation. As shown in Figure 3B, EJP amplitudes in *tweek* mutants declined to about 55%–60% of the initial response when stimulated at 10 Hz in 5 mM Ca^{2+}. In contrast, controls maintained release at about 90% of the initial response after 10 min at 10 Hz (Figure 3B). The inability of *tweek* mutants to maintain normal levels of transmission during intense activity is consistent with a defect in vesicle trafficking or recycling.

Tweek Is Required in Neurons for Proper FM1-43 Dye Uptake

Synaptic vesicle density in *tweek* mutant PRs is lower than in controls (Figure 1), suggesting a defect in maintaining a normal synaptic vesicle pool. To assess if vesicle recycling is affected, we performed live imaging with FM1-43 dye at third instar NMJs (Ramaswami et al., 1994). In aqueous environments, FM1-43 is nonfluorescent, but when bound to membranes it increases its fluorescence quantum yield. Hence, newly endocytosed vesicles in the presence of FM1-43 will be fluorescently labeled, providing a quantitative measure of vesicle uptake (Betz and Bewick, 1992; Verstreken et al., 2007). As shown in Figures 3C, 3D, and S4C, and S4D, when controls, including *tweek* mutants that carry the genomic rescue construct, are stimulated for 1 min with 90 mM KCl or for 10 min with 10 Hz nerve stimulation in the presence of FM1-43, synapses are brightly labeled, indicating efficient vesicle retrieval from the membrane during stimulation. In contrast, *tweek* mutant synapses are labeled less.

To test if this defect is caused by loss of *tweek* in motor neurons we expressed different RNAi constructs (VDRC) (Dietzl et al., 2007) against *tweek*. RT-PCR and quantitative RT-PCR show that expression of three RNAi constructs leads to decreased *tweek* mRNA levels (Figure S5 and data not shown). We stimulated synapses of animals that express these RNAi constructs in neurons using *nsyb-GAL4* for 1 min in 90 mM KCl and assessed FM1-43 dye uptake efficiency. As shown in Figures 3E and 3F, expression of *8060GD (CG15133)*, *19305GD (CG15134)*, or *19306GD (CG15134)* results in a significant reduction of FM1-43 dye uptake, whereas expression of RNAi constructs that do not significantly affect *tweek* expression show normal uptake. These data indicate that *tweek* acts in the presynaptic neuron and are consistent with an endocytic defect and/or a reduced synaptic vesicle pool.

tweek Affects Synaptic Vesicle Density and Size

To further explore presynaptic defects in *tweek* mutants we performed TEM at third instar NMJ boutons. As shown in Figure 4, synaptic vesicle number is reduced in *tweek* mutant boutons.
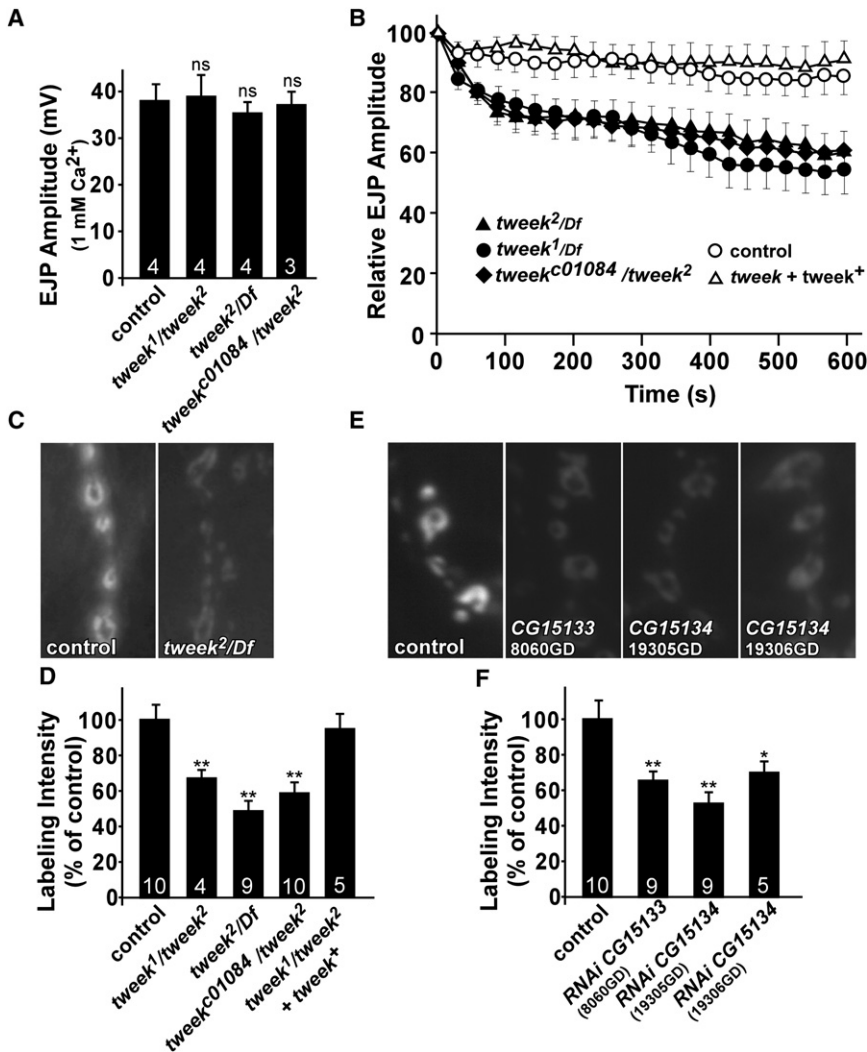
Figure 3. Synaptic Vesicle Endocytosis Is Impaired in *tweek* Mutants

(A) Average EJP amplitude recorded in 1 mM Ca^{2+} in controls, $tweek^1/tweek^2$, $tweek^2/Df$, and $tweek^{c01084}/tweek^2$. Recordings were performed for 1 min at 1 Hz and 60 EJP amplitudes were averaged per recording. Under these conditions, there are no exocytic defects in *tweek* mutants. Error bars: standard error of the mean (SEM); n (the numbers of animals tested) are indicated; t test; ns: not significant.

(B) Average EJP amplitudes recorded at 10 Hz for 10 min in 5 mM external Ca^{2+} in controls, $tweek^1/Df$, $tweek^2/Df$, $tweek^{c01084}/tweek^2$, and $tweek^1/tweek^2$; $tweek^+(HB69)$ rescued animals. Average EJP amplitudes (binned per 30 s) are normalized to the initial response (an average of the first 5 EJPs). Error bars: SEM.

(C–F) FM1-43 dye uptake in controls ($y\ w$; $P\{y^+\}$ FRT40A) (C and D) or ($UAS\text{-}DCR2/w^{1118}$; nsyb-GAL4/+) (E and F), $tweek^1/tweek^2$ mutants ($y\ w$ eyFLP; $tweek^1$ $P\{y^+\}$ FRT40A/$tweek^2$ $P\{y^+\}$ FRT40A), $tweek^2/Df$ mutants ($y\ w$ eyFLP; $tweek^2$ $P\{y^+\}$ FRT40A/Df(2L)Exel8036), $tweek^{c01084}/tweek^2$ mutants ($y\ w$ eyFLP; $tweek^2$ $P\{y^+\}$ FRT40A/$tweek^{c01084}$), $tweek^1/tweek^2$ mutants with a rescue construct ($y\ w$ eyFLP; $tweek^1$ $P\{y^+\}$ FRT40A/$tweek^2$ $P\{y^+\}$ FRT40A; $tweek^+(HB69)$/+) (C and D), and flies that express RNAi directed against *tweek* ($UAS\text{-}DCR2/w^{1118}$; 8060GD/+; nsyb-GAL4/+ or $UAS\text{-}DCR2/w^{1118}$; nsyb-GAL4/19305GD or 19306GD) (E and F). Preparations were incubated in 4 μM dye and were stimulated with 1 min of 90 mM KCl to label the exo-endo cycling pool. Error bars: SEM; n (the numbers of animals tested) are indicated; t test: *p < 0.05; **p < 0.01.

While many synaptic features such as mitochondrial number or structure (Figures 4A–4C and 4G), dense body number (T-bars) (Figures 4H and 4I), dense body morphology (Figures 4E and 4F), and the number of docked synaptic vesicles within a 200 nm radius around dense bodies (Figures 4E, 4F, and 4J) appear normal in *tweek* mutants compared to controls, vesicle counts reveal ∼64% fewer vesicles per unit area (Figures 4A–4D and 4K). *tweek* boutons also contain more large-diameter vesicles than controls: the diameters of synaptic vesicles are typically <50 nm in controls (Figures 4A, 4L, and 4M), but *tweek* mutants contain numerous vesicles and cisternae that exceed this diameter (Figures 4B–4D, 4L, and 4M). Hence, loss of Tweek, similar to endocytic mutants *AP180/lap*, *dap160*, *eps15*, and *stoned* (Chen et al., 1998; Fergestad et al., 1999; Gonzalez-Gaitan and Jackle, 1997; Stahelin et al., 2003; Stimson et al., 2001; Zhang et al., 1998), leads to reduced vesicle density and causes the formation of larger and more heterogeneously sized vesicles.

The fusion of large synaptic vesicles should lead to an increased amount of neurotransmitter released per single vesicle fusion event (Zhang et al., 1998). We therefore recorded spontaneous vesicle fusion events (minis) in current clamp mode (miniature excitatory junctional potentials—mEJPs) (Figure 5A) as well as in voltage clamp mode (miniature excitatory junctional currents—mEJCs) (Figures 5B, 5C, and 5F). As shown in a cumulative probability plot of mEJP amplitudes (Figure 5A) or by calculating the average mEJP (not shown) and mEJC amplitudes (Figure 5B), mini amplitudes in *tweek* mutants are larger compared to controls. In addition, we also find a significant reduction in mini frequency (Figure 5C). These data suggest that single vesicle fusions can elicit larger responses in *tweek* mutants compared to controls. Since GluRIIA and GluRIIC/III immunohistochemical staining of postsynaptic glutamate receptors (Marrus et al., 2004; Schuster et al., 1991) does not show differences in receptor cluster size or cluster intensity between *tweek* and controls (GluRIIC/III cluster intensity in control: 100% ± 8.0% and in $tweek^1/tweek^2$: 88.8% ± 1.5%, t test: p = 0.29), synaptic vesicles in *tweek* mutants release abnormally large quantities of neurotransmitters in agreement with an increased vesicle size in the mutants.
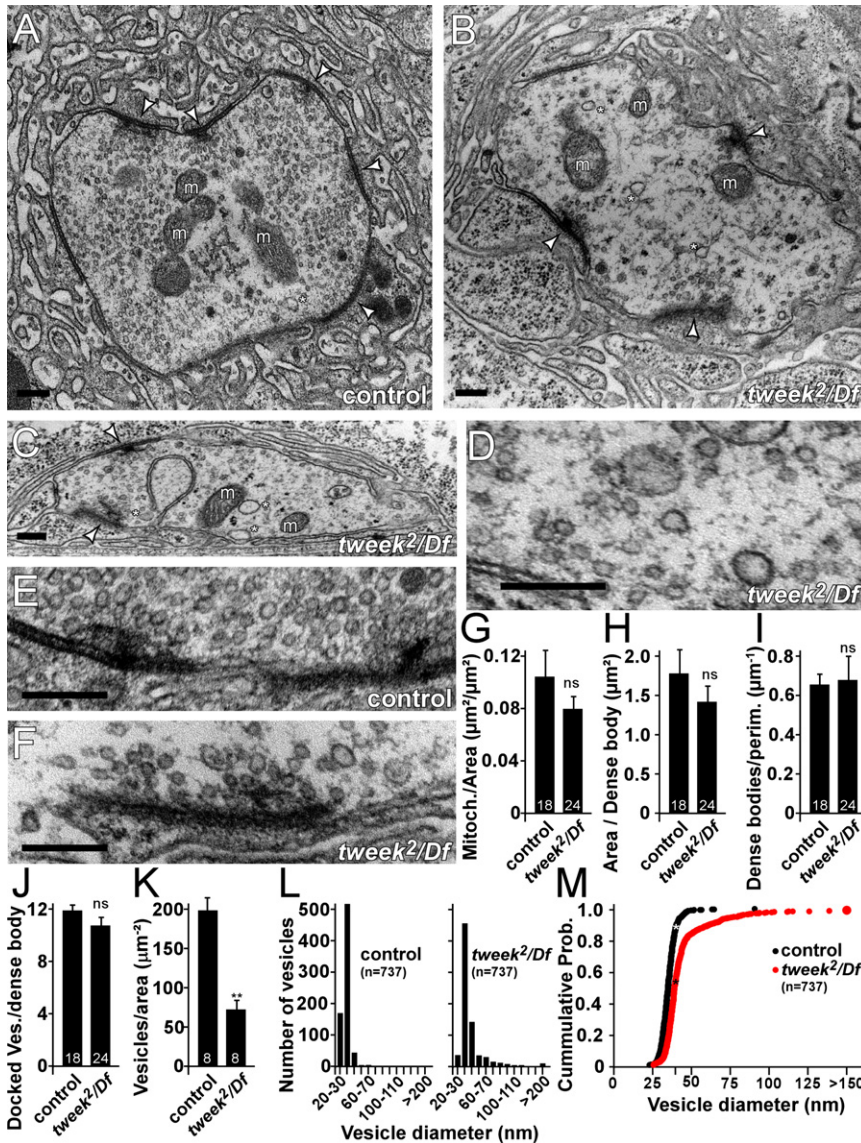
Figure 4. Vesicle Size and Number Are Altered in *tweek* Mutants

(A–F) Ultrastructure of control (*y w; P{y+} FRT40A*) (A and E) and *tweek2/Df* (*y w eyFLP; tweek2 P{y+} FRT40A/Df(2L)Exel8036*) mutants (B–D and F), NMJ boutons (A–D), and dense bodies (E–F). Note the reduced synaptic vesicle density and the heterogeneity in synaptic vesicle size (asterisks) in the mutants compared to the control. Dense bodies (arrowheads) and mitochondria (m) are marked. Scale bars are 200 nm.

(G–K) Quantification of ultrastructural features: mitochondrial density (G), boutonic area per dense body (H), dense bodies per perimeter bouton (I), number of docked vesicles synaptic in a 200 nm radius around the dense body (J), and synaptic vesicle density (K). **p < 0.01 (t test); ns, not significant; Error bars: SEM. The numbers of analyzed sections are indicated in the bars, and images were acquired from eight boutons in five different animals.

(L and M) Histograms of synaptic vesicle diameter in controls and *tweek2/Df* and cumulative histogram of synaptic vesicle diameters indicating larger vesicles in *tweek* mutants. Seven hundred and thirty-seven vesicle diameters were measured for each genotype.

Proteins Required for Proper Clathrin Coat Assembly Are Decreased at *tweek* NMJs

α-adaptin, AP180/Lap, and Stoned B are adaptor-like proteins that have been implicated in early steps of vesicle recovery, and mutations in the genes that encode these proteins lead to phenotypes that are qualitatively similar to *tweek* (Fergestad et al., 1999; Gonzalez-Gaitan and Jackle, 1997; Stimson et al., 2001; Zhang et al., 1998). We therefore assessed the levels of these proteins in *tweek* mutant boutons (*tweek2/Df(2L)Exel8036*, *tweek1/tweek2*, and for α-adaptin also *tweek2/tweekc01084*). The levels of these proteins are markedly reduced in *tweek* NMJ boutons (Figures 6A–6C and 6G and data not shown). This decrease is not due to reduced expression levels of these proteins, as western blots using whole larval extracts did not show obvious differences between *tweek* and controls (Figure 6I and quantification in the legend).

To assess if *tweek* mutations affect the localization of other endocytic proteins we labeled NMJs with antibodies against Dynamin (van der Bliek and Meyerowitz, 1991), Dap160, Eps15 (Koh et al., 2004; Majumdar et al., 2006; Marie et al., 2004; Roos and Kelly, 1999), and Endophilin (Verstreken et al., 2002). As shown in Figures 6D–6F and 6H, *tweek* does not affect the level or localization of these proteins. In summary, Tweek mediates the normal recruitment, retention, and/or stability of several endocytic adaptor-like proteins that are intrinsic components of the clathrin coat.

EJP amplitudes are similar in controls and *tweek* mutants but mini amplitudes are not. Hence, the number of vesicles released per stimulus (quantal content) is likely altered in *tweek*, possibly as a result of homeostatic regulation (Davis, 2006). To calculate the quantal content we recorded EJC amplitudes in 1 mM Ca2+ (Figures 5D and 5E) and divided the average EJC amplitude by the average mEJC amplitude (quantal amplitude; Figure 5B). Our data indicate that the quantal content in *tweek* is reduced by 31%–37% compared to controls (Figure 5G). However, as vesicles in *tweek* are larger, the amount of membrane added per stimulus is comparable or even slightly increased in *tweek* when compared to controls (Figure 5H). Hence, during stimulation, mutants and controls release similar amounts of synaptic vesicle membrane. Since FM1-43 dye uptake is reduced, these data further support a defect in endocytosis or recycling in *tweek* mutants.
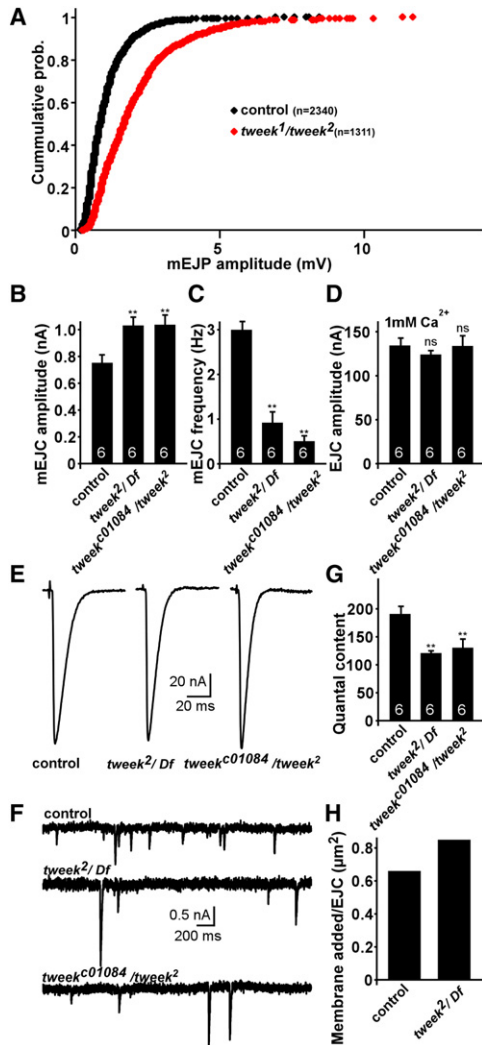
Figure 5. Quantal Size Is Increased in *tweek* Mutants

(A) Cumulative histogram of mEJPs measured from controls (black: *y w; P{y+} FRT40A*) and *tweek1/tweek2* (red: *y w eyFLP; tweek1 P{y+} FRT40A/tweek1 P{y+} FRT40A*) animals. Note the rightward shift in *tweek* mutants signifying larger mEJP amplitudes.

(B and C) Average mEJC amplitude (B) and frequency (C) in controls and *tweek* mutants (*tweek2/Df*: *y w eyFLP; tweek2 P{y+} FRT40A/Df(2L)Exel8036* and *tweekc01084/tweek2*: *y w eyFLP; tweek2 P{y+} FRT40A/tweekc01084*). Error bars: SEM; *n* (the numbers of animals tested) are indicated; t test: *p < 0.05; **p < 0.01; ns: not significant.

(D) Average EJC amplitude in controls and *tweek* mutants recorded in 1 mM extracellular Ca^{2+}. Error bars: SEM; *n* (the numbers of animals tested) are indicated; t test; ns: not significant.

(E and F) Sample EJC (E) and mEJC (F) traces recorded from controls and *tweek* mutants. Recordings were performed for 1 min at 0.1 Hz and all EJC amplitudes were averaged per recording.

(G) Junctional quantal content at 1 mM Ca^{2+} calculated by dividing the average EJC amplitude by the average mEJC amplitude. Error bars: SEM; *n* (the numbers of animals tested) are indicated; t test: **p < 0.01.

(H) Estimation of vesicular membrane added per stimulus in 1 mM extracellular Ca^{2+} calculated by multiplying the quantal content (control: 189 quanta; *tweek2/Df*: 120 quanta) by the average vesicle surface area based on TEM in Figure 4 (control: vesicle radius 16.7 nm; *tweek2/Df*: vesicle radius 23.8 nm).

PI(4,5)P$_2$ Availability Is Reduced at *tweek* NMJs

Several endocytic adaptors have been shown to interact with phosphorylated inositides (e.g., PI(4,5)P$_2$—reviewed in Lemmon, 2003; Wenk and De Camilli, 2004). One possibility therefore is that Tweek affects the levels or distribution of synaptic PIs, thought to be critical for vesicle recycling (Cremona et al., 1999; Di Paolo et al., 2004; Micheva et al., 2001; Verstreken et al., 2003). To estimate the PI levels at *tweek* NMJ boutons we expressed a PI-interacting protein domain fused to EGFP that reports PI(4,5)P$_2$ levels in vivo (Jost et al., 1998; Varnai and Balla, 2006).

To visualize PI(4,5)P$_2$ we cloned an EGFP-fused pleckstrin homology (PH) domain of PLCδ1, known to bind PI(4,5)P$_2$ (Varnai and Balla, 1998), in *pUAST* and expressed it using the *UAS-GAL4* system. To test the specificity of this probe, we also expressed a mutant PLCδ-PH^{mut}-EGFP that cannot bind PI(4,5)P$_2$ (Varnai and Balla, 2006). As shown in Figure S6A, the wild-type PLCδ-PH-EGFP probe decorates the membrane in salivary gland cells, whereas the mutant PLCδ-PH^{mut}-EGFP is diffusely present in the cytoplasm and concentrates in the nucleus (Figure S6B). Furthermore, in neurons of the larval ventral nerve cord and in the adult brain, PLCδ-PH-EGFP is present in the neuropil synapses (Figure S6C). In contrast, the mutant PLCδ-PH^{mut}-EGFP is diffusely present in the cytoplasm, labeling mostly the cell bodies and less the neuropil (Figure S6D and data not shown). These data indicate that in *Drosophila* the PLCδ-PH-EGFP probe is enriched at synapses (Micheva et al., 2001).

To explore possible changes in levels or distribution of PI(4,5)P$_2$ at the NMJ, we used *elav-GAL4* to express the PLCδ-PH-EGFP probe in the nervous system of *tweek* mutants and wild-type controls. In wild-type controls the probe is present at synaptic boutons and enriched on their membranes (Figure 7A). We also expressed the probe in *synj* mutants as a positive control to assess the ability of the probe to reveal changes in PI(4,5)P$_2$. Synj is a presynaptic phosphoinositide phosphatase, and mouse as well as fly *synj* mutants show an overall increase in the concentration of PI(4,5)P$_2$ (Cremona et al., 1999; Voronov et al., 2008; L.E.S. and P.D.C., unpublished data). In agreement with these observations, the signal produced by PLCδ-PH-EGFP at *synj1* mutant synapses is increased (Figures 7B and 7D). In contrast to *synj* and to controls, the levels of PLCδ-PH-EGFP fluorescence expressed using *elav-GAL4* are decreased in *tweek* mutants (Figures 7C, 7D, and S7). This difference is not due to an effect of *tweek* on GFP fluorescence as the levels and localization of untagged GFP, expressed in neurons, are not significantly different in *tweek* versus controls (Figures 7M and 7N). Hence, these results suggest that Tweek is required to maintain normal levels or availability of PI(4,5)P$_2$ at *Drosophila* NMJs.

To analyze the dynamics of PI(4,5)P$_2$ localization in control and *tweek* mutants during vesicle cycling we performed live imaging of PLCδ-PH-EGFP driven by the strong neuronal *nsyb-GAL4* driver, while stimulating the motor nerve for 100 s at 20 Hz. In controls, PLCδ-PH-EGFP distribution during stimulation shows no obvious changes when compared to synapses at rest whereas the PLCδ-PH-EGFP distribution in *tweek* mutants shows obvious differences (Figures 7E–7H). Prior to stimulation the distribution of PLCδ-PH-EGFP in controls and *tweek* mutants
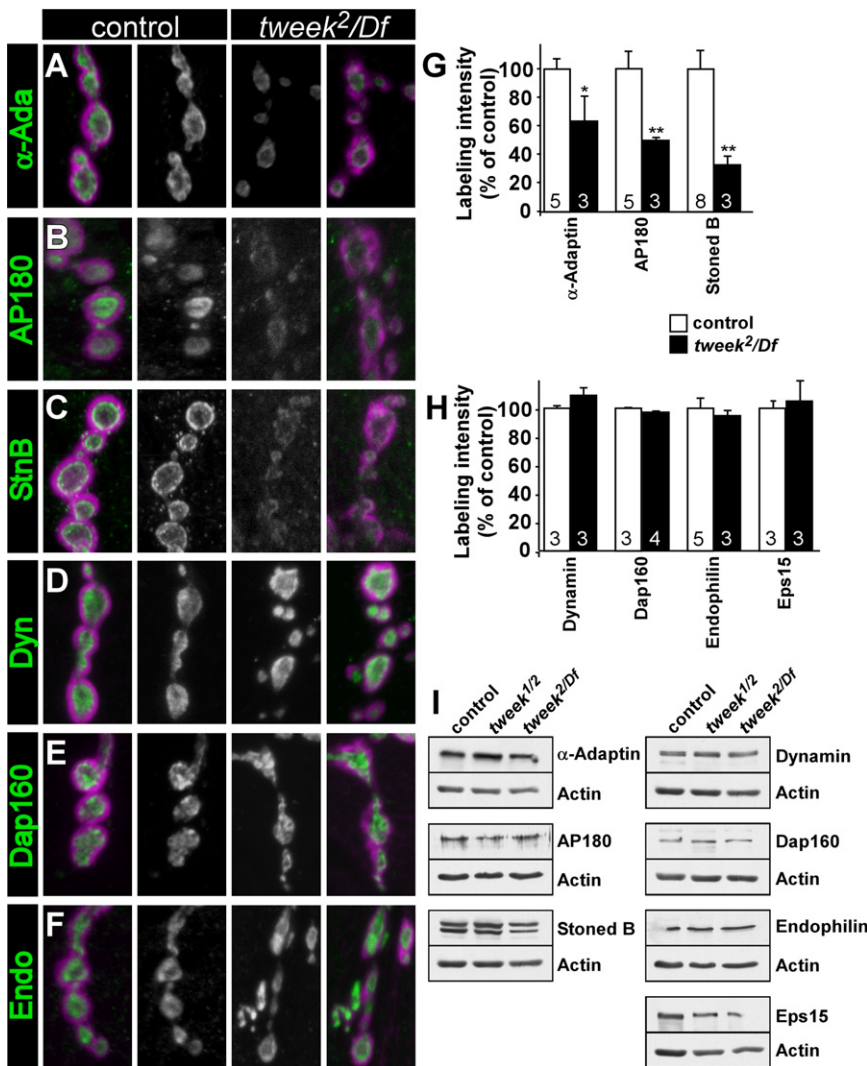
Figure 6. Endocytic Adaptor Proteins Are Destabilized at *tweek* Mutant Boutons

(A–F) Confocal images showing labeling of control (*y w; P{y+} FRT40A*) (left) and *tweek2/Df* (*y w eyFLP; tweek2 P{y+} FRT40A/Df(2L)Exel8036*) (light) larval filets with α-adaptin (A), AP180/Lap (B), Stoned B (C), Dynamin (D), Dap160/Intersectin (E), Endophilin (F) (green), and DLG/PSD-95 (magenta). Green channel labeling for control and *tweek2/Df* is shown in the middle (gray scale).

(G and H) Quantification of boutonic labeling intensity (inside the respective DLG circumscribed areas) for markers shown in (A)–(F) and for Eps15. Data for *tweek1/tweek2* mutants (*y w eyFLP; tweek1 P{y+} FRT40A/tweek2 P{y+} FRT40A*) are very similar to that for *tweek2/Df* mutants (not shown). *p < 0.05, **p < 0.01 (t test); Error bars: SEM; *n* (the numbers of animals labeled) are indicated in the bars. Error bars: SEM; *n* (the numbers of animals tested) are indicated; t test: *p < 0.05; **p < 0.01.

(I) Western blots of larval extracts of controls, *tweek1/tweek2*, and *tweek2/Df* using antibodies against the endocytic proteins tested in (A)–(H). Protein loading amounts were tested with anti-actin antibodies. Quantification of three independent westerns normalized to actin loading control (values relative to control levels): α-adaptin: control: 100.0% ± 12.7%; *tweek1/tweek2*: 95.8% ± 19.1%; *tweek2/Df(2L)Exel8036*: 86.4% ± 20.3%; *p:*ns. Lap/AP180: control: 100.0% ± 6.4%; *tweek1/tweek2*: 94.2% ± 8.9%; *tweek2/Df(2L)Exel8036*: 82.3% ± 21.2%; p:ns. Stoned B: control: 100.0% ± 23.0%; *tweek1/tweek2*: 87.4% ± 15.3%; *tweek2/Df(2L)Exel8036*: 81.5% ± 2.4%; *p:*ns.

are similar. Note, however, that the levels of PLCδ-PH-EGFP are decreased when compared to controls (Figures 7E–7H). During stimulation, PLCδ-PH-EGFP redistributes and concentrates in presynaptic clusters in *tweek* mutants, while the mutant PLCδ-PHmut-EGFP probe does not concentrate in such clusters (Figures 7H, 7H′, and 7H″ and data not shown). These structures in *tweek* mutants often persist for ~100 s after cessation of the stimulation (Figures 7I and 7J). The clusters may represent lingering endocytic intermediates that still harbor $PI(4,5)P_2$. Hence, the data suggest that Tweek affects not only the basal levels of $PI(4,5)P_2$ but also its synaptic distribution during neuronal activity.

To test if Tweek affects the availability of other PIs we also expressed 2xFYVE-EGFP, a marker for PI(3)P in the nervous system (Wucherpfennig et al., 2003). PI(3)P is enriched on endosomes, but limited amounts may also be present on the plasma membrane. However, the expression of 2xFYVE-EGFP in controls and *tweek* mutants is not significantly different (Figures 7K and 7L), indicating that *tweek* does not affect the localization or abundance of PI(3)P.

Synaptojanin Mutations Partially Suppress Endocytic Defects in *tweek*

To provide additional in vivo evidence that the availability of $PI(4,5)P_2$ is reduced in *tweek*, we tested vesicle uptake in *tweek* mutants with reduced PI phosphatase activity by removing one copy of *synj*. Removal of a single copy of *synpatojanin* may elevate the reduced $PI(4,5)P_2$ levels observed in *tweek* mutants, providing strong genetic evidence for a direct link of Tweek to vesicle recycling and PIPs. To assess endocytosis in these animals, we stimulated synapses for 5 min with KCl in the presence of FM1-43 and measured labeling intensity. Using this protocol, dye uptake in *synj*/+ heterozygotes and controls is indistinguishable, indicating no dominant effect of the *synj1* mutation on endocytosis (Figures 8A and 8D). Interestingly, *tweek* mutants that lack one copy of *synj* (*tweek1 synj1/tweek2* or *tweek2 synj1/ Df(2L)Exel8036*) take up significantly more dye than *tweek* mutants (*tweek1/tweek2* or *tweek2/Df(2L)Exel8036*) (Figures 8B–8D). However, dye uptake in *tweek* mutants that are heterozygous for *synj* is still less than in controls (*eyFLP; FRT40A*) or in *synj*/+. These data indicate that the levels of $PI(4,5)P_2$ can be genetically manipulated to affect FM1-43 dye uptake.

We also tested if the removal of one copy of *synj* in *tweek* mutants partially restores α-adaptin levels in boutons. While
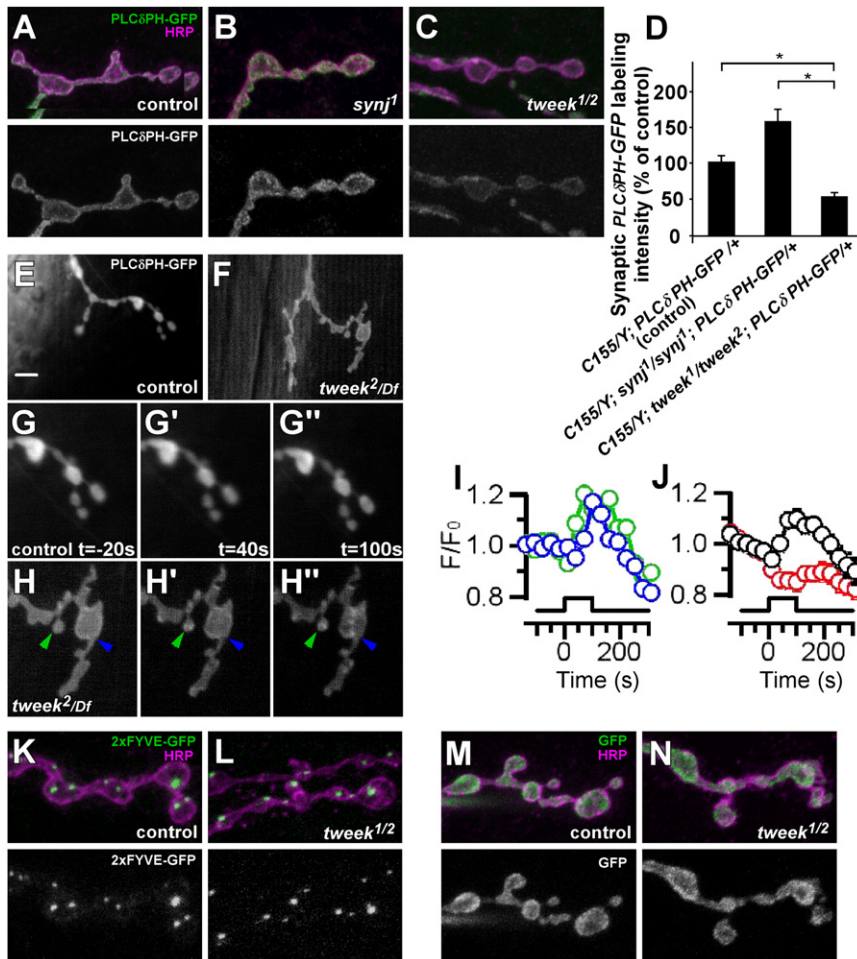
Figure 7. Synaptic PI(4,5)P$_2$ Levels Are Reduced in *tweek* Mutants

(A–C) Neuronal PI(4,5)P$_2$ levels in boutons of control (*elav-GAL4/Y; UAS-PLCδ-PH-EGFP/+*), *synj^1* (*elav-GAL4/Y; FRT42D synj^1; UAS-PLCδ-PH-EGFP/+*), and *tweek^1/tweek^2* (*elav-GAL4/Y; tweek^1 P{y$^+$} FRT40A/tweek^2 P{y$^+$} FRT40A; UAS-PLCδ-PH-EGFP/+*) third instar filets were visualized by a PLCδ-PH-EGFP probe (green). Neuronal membranes were counterstained with anti-HRP (magenta). Green channel is separately shown on the bottom. Note increased EGFP levels in *synj^1* mutants and decreased EGFP levels in *tweek* mutants.

(D) Quantification of PLCδ-PH-EGFP intensity shown in (A)–(C) inside the volume demarcated by anti-HRP labeling in the indicated genotypes. Error bars: SEM; *p < 0.05 (t test).

(E–H) Live imaging of PLCδ-PH-EGFP localization before (E, F, G, and H) and after 40 s (G′ and H′) or 100 s (G″ and H″) of 20 Hz stimulation of (E and G–G″) control (*y w/w; FRT40A/+; UAS-PLCδ-PH-EGFP, nsyb-GAL4/+*) and (F and H–H″) *tweek^2/Df* (*y w/w; tweek^2 FRT40A/Df(2L)Exel8036; UAS-PLCδ-PH-EGFP, nsyb-GAL4/+*) third instar NMJs. GFP imaging was performed with a CCD camera, and (G) and (H) are magnifications of (E) and (F), respectively. Controls never show PLCδ-PH-EGFP clusters (n = 7 animals) whereas numerous PLCδ-PH-EGFP clusters (green and blue arrowheads) appear in *tweek* mutants during stimulation. Such clusters are not observed using the PLCδ-PH^{mut}-EGFP, indicating specificity. Scale bar: 5 μm.

(I and J) Quantification of the fluorescence of PLCδ-PH-EGFP clusters during stimulation (start at t = 0, marked by the bar). (I) Green and blue traces show the normalized fluorescence of individual clusters indicated in (H–(H″), showing that some clusters form early in the stimulus (green) and others form later (blue). Note also that clusters remain for an extended period of time (>100 s) following stimulation before they disappear. (J) Black trace shows the average ± SEM for all clusters formed in the *tweek^2/Df* experiments (23 clusters, 4 animals). The red trace shows the corresponding change in fluorescence in the remainder of the terminal of *tweek^2/Df*, and this trace appears very similar to the one measured from control boutons where also no clusters were observed (G–G″).

(K and L) Neuronal PI(3)P levels in boutons of control (*elav-GAL4/Y; UAS-2xFYVE-EGFP/+*) or *tweek^1/tweek^2* mutant (*elav-GAL4/Y; tweek^2 UAS-2xFYVE-EGFP/tweek^1 P{y$^+$} FRT40A*) third instar filets were visualized with a 2xFYVE-EGFP probe (green). Neuronal membranes were counterstained with anti-HRP (magenta). Green channel is separately shown on the bottom.

(M and N) Neuronal GFP levels in boutons of control (*elav-GAL4/Y; UAS-GFP/+*) or *tweek^1/tweek^2* mutant (*elav-GAL4/Y; tweek^2 UAS-GFP/tweek^1 P{y$^+$} FRT40A*) third instar filets (green). Neuronal membranes were counterstained with anti-HRP (magenta). Green channel is separately shown on the bottom.

tweek mutants (*tweek^1/tweek^2*, *tweek^2/Df(2L)Exel8036*, or *tweek^2/tweek^{c01084}*) show reduced α-adaptin levels in synaptic boutons (Figures 6A, 6G, 8F, and 8H), removing one copy of *synj* (*tweek^1 synj^1/tweek^2*, *tweek^2 synj^1/Df(2L)Exel8036* or *tweek^2 synj^1/tweek^{c01084}*) partially restores α-adaptin levels (Figures 8E–8H). Hence, levels of an endocytic adaptor protein in *tweek* mutant NMJ synapses can be restored by decreasing phosphoinositide dephosphorylation activity, consistent with the observation that the availability of phosphorylated inosities is reduced in *tweek* mutants.

DISCUSSION

In an unbiased genetic screen to identify genes that affect neuronal communication we have identified mutants that affect different aspects of synaptic function (Hiesinger et al., 2005; Koh et al., 2004; Verstreken et al., 2003). In the same screen, we also identified *tweek*, which encodes a very large protein without established protein motifs. Interestingly, a *C. elegans tweek* homolog, *lpd-3*, which encodes the carboxy-terminal end of Tweek but is most likely part of a much larger gene (including Y47G6A.23 and Y47G6A.29), was previously identified in an RNAi screen for lipid storage defects (McKay et al., 2003). However, the molecular nature underlying the RNAi phenotype in worms has not been investigated. Our data indicate that *tweek* plays a role in synaptic vesicle recycling likely by regulating PI-lipid signaling at the synapse.

The Tweek protein is unusually large as it encodes a protein of 5076 amino acids. Interestingly, Tweek does not contain any known motifs, and hence cloning of the gene did not reveal
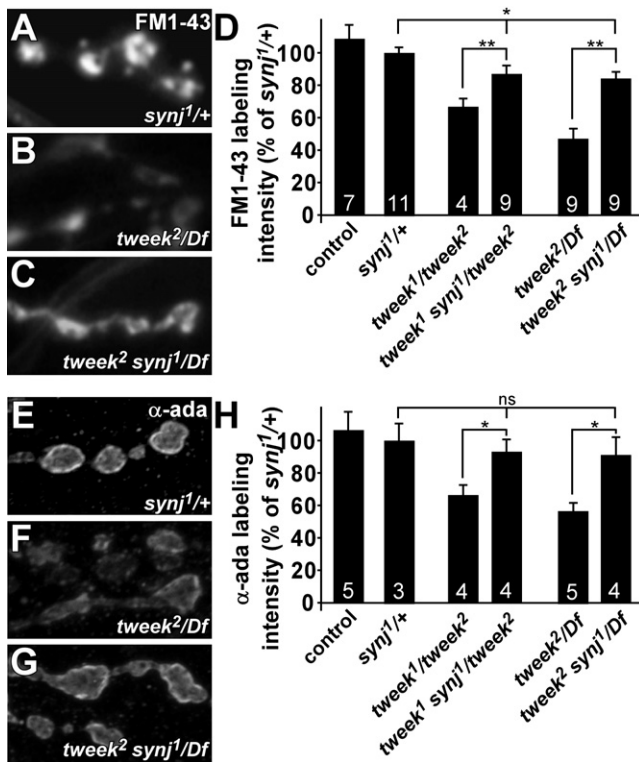
Figure 8. Removal of a Single Mutant Copy of *synaptojanin* Suppresses Endocytic Defects in *tweek*

(A–D) FM1-43 dye uptake experiment on *synj[1]*/+ controls (*y w ey-FLP*; *FRT42D synj[1]/FRT42D*), *tweek[2]/Df* mutants (*y w eyFLP*; *tweek[2] P{y[+]} FRT40A/ Df(2L)Exel8036*), and *tweek[2]/Df* mutants that lack one functional copy of the *synj* gene (*y w eyFLP/y w*; *tweek [2] synj[1]/Df(2L)Exel8036*). Preparations were stimulated in 90 mM KCl for 5 min, washed, and imaged (A–C) and labeling intensity quantified (D). Dye uptake in *synj[1]*/+ and *y w eyFLP; FRT40A* controls is indistinguishable (shown in D). Error bars: SEM; *n* (the numbers of animals tested) are indicated; t test: *p < 0.05; **p < 0.01. Note the increased FM1-43 dye uptake in *tweek* mutants with reduced *synj* function compared to *tweek* mutants. To measure PI(4,5)P$_2$ levels in *synj[1]* and *synj[1]*/+ animals we expressed the PLCδ-PH-EGFP probe and measured boutonic fluorescence relative to controls: 100% ± 12% for controls (*elav-GAL4/Y; UAS-PLCδ-PH-EGFP/+*); 157% ± 20%, p < 0.05 for *synj[1]* (*elav-GAL4/Y; FRT42D synj[1]; UAS-PLCδ-PH-EGFP/+*); 117% ± 8%, p < 0.1 for *synj[1]*/+ (*elav-GAL4/Y; FRT42D synj[1]*/+; *UAS-PLCδ-PH-EGFP/+*).

(E–H) α-adaptin labeling in *synj[1]*/+ controls, *tweek[2]/Df* mutants, and *tweek[2]/Df* mutants that lack one functional copy of the *synj* gene (*tweek[2] synj[1]/Df*). (H) Quantification of α-adaptin labeling intensity. Error bars: SEM; *n* (the numbers of animals tested) are indicated; t test: *p < 0.05; ns: not significant. α-adaptin labeling in *synj[1]*/+ and *y w; P{y[+]} FRT40A* controls is indistinguishable (shown in H). Note the increased α-adaptin labeling in *tweek* mutants with reduced *synj* function compared to *tweek* mutants. *p < 0.05, **p < 0.01 (t test); Error bars: SEM; *n* (the numbers of animals labeled) are indicated in the bars.

any hints about its potential function or localization. Note that the three CGs that form the *tweek* transcript are also found clustered in other species. These *tweek* homologs have most likely been wrongly annotated in almost all species (except human) as separate genes. No full-length cDNA has been reported in any species, and when expression patterns of portions of the *tweek* homologs are available, they are localized in the nervous system

and fat tissue (Chintapalli et al., 2007; Manak et al., 2006; McKay et al., 2003). In flies, the *tweek* RNA transcript is also expressed in the CNS, but localization of the protein could not be established as we were unable to raise an antibody upon injection of various antigens in ten animals. Similarly, localization of the protein using a mCherry-tagged genomic construct that can rescue the *tweek* mutations failed, even when we tried to enhance signal using antibodies against the tag (data not shown). Taken together these data suggest that the protein derived from the *tweek* locus is not abundant, and this may explain why it has not been identified previously through biochemical approaches.

tweek mutants harbor the hallmarks of mutants that affect endocytosis. Electrophysiological analyses show that *tweek* mutants fail to maintain neurotransmitter release during intense stimulation and internalize less FM1-43 dye, indicating a smaller vesicle pool. They also display reduced synaptic vesicle numbers and aberrantly large vesicles. We used Synapto-pHluorin (Poskanzer et al., 2003) to further test membrane recycling following stimulation (0.2 s at 50 Hz) but observed only a slightly slower and statistically insignificant decay in fluorescence quenching in *tweek* mutants compared to controls. While these data suggest that part of the recycling defect in *tweek* mutants may occur after newly endocytosed vesicles are acidified, we also did not observe a difference in SynaptopHluorin fluorescence decay in *dap160* endocytic mutants as compared to controls when stimulated using the same paradigm (Figure S8). These data suggest that SynaptopHluorin may not be able to detect the defects in membrane recycling in these "endocytic" mutants.

While some of the phenotypes we observe in *tweek* mutants may be recapitulated in other fly mutants (Daniels et al., 2004, 2006), the *tweek* mutants are phenotypically much more similar to mutants that affect endocytosis. Indeed, *stoned*, *AP180/lap*, *dap160*, and *eps15* mutants all exhibit reduced vesicle numbers (Fergestad et al., 1999; Ferguson et al., 2007; Koh et al., 2004; Majumdar et al., 2006; Marie et al., 2004; Nonet et al., 1999; Stimson et al., 2001; Zhang et al., 1998). These phenotypes combined with the aberrant localization of endocytic adaptor proteins in *tweek* mutants are consistent with the hypothesis that Tweek at least in part affects vesicle recycling early, when adaptor proteins are recruited to the plasma membrane, and this is bolstered by the dominant genetic interaction with *synj*. However, we cannot exclude additional roles for the protein at later steps of the vesicle cycle.

Both synaptic vesicle exocytosis and endocytosis are critically dependent on PIs present at synaptic membranes (Di Paolo et al., 2004; Schiavo et al., 1996; Verstreken et al., 2003). PI(4,5)P$_2$ in the plasma membrane is thought to be a major anchor point for endocytic adaptor proteins that link clathrin to this membrane (Cremona et al., 1999; Gaidarov et al., 1996). Reduced availability of PI(4,5)P$_2$ in *tweek* mutants may lead to reduced coat nucleation at the synapse and therefore provides a rationale for the mislocalization of endocytic adaptor proteins in the mutants. While a biochemical link between Tweek, phosphoinositide availability, and adaptor localization awaits further investigation, our model is consistent with the observation that increasing the PI(4,5)P$_2$ levels in *tweek* mutants, by reducing

synj expression, partially restores the localization of the AP2 adaptor. Note that not all PI(4,5)P$_2$-interacting proteins are destabilized at *tweek* mutant synapses. For example, Dynamin binds PI(4,5)P$_2$, yet, it seems to be localized similarly in *tweek* and controls. Furthermore, the levels of Synaptotagmin, a synaptic vesicle protein known to interact with PI(4,5)P$_2$, appears similar in controls and *tweek* mutants (data not shown). We surmise that while PI binding may be mediating the function of these proteins (Achiriloaie et al., 1999; Bai et al., 2004; Zoncu et al., 2007), they may require less PI(4,5)P$_2$ than adaptor proteins.

Although a large body of evidence demonstrates a role for PI(4,5)P$_2$ in various cellular processes (Hassan et al., 1998; Horn, 2005; York, 2006), *tweek* mutant cells do not show signs of major cellular dysfunction beyond a defect to maintain synaptic transmission, indicating that the effect of *tweek* loss of function in neurons is rather specific to synaptic vesicle recycling. We and others have observed a similar remarkably specific phenotype in *synj* mutants (Cremona et al., 1999; Harris et al., 2000; Van Epps et al., 2004; Verstreken et al., 2003). Although *synj* mutants lead to an increase in phosphorylated PIs, defects at the NMJ appear to be specific to synaptic vesicle endocytosis. Hence, specific factors locally regulate the availability of specific PI lipids, even within the synapse. As a result, PI phosphatases, kinases, and proteins like Tweek that may control PI availability must play important roles during vesicle recycling.

EXPERIMENTAL PROCEDURES

Genetics and Molecular Biology

Throughout the paper, control animals were isogenized *y w; P{y$^+$, ry$^+$}25F P{neoFRT}40A* unless otherwise indicated, and *tweek^1* or *tweek ^{2}* mutants were *y w P{ey-FLP} P{GMR-lacZ} (abbreviated y w eyFLP); tweek^1 P{y$^+$, ry$^+$}25F P{neoFRT}40A* and *y w P{ey-FLP} P{GMR-lacZ}; tweek^2 P{y$^+$, ry$^+$}25F P{neoFRT}40A*. Additional details on *tweek* alleles and identification of the *tweek* gene as well as generation of transgenic animals appear in the Supplemental Experimental Procedures.

Immunohistochemistry and Western Blotting

Labeling was performed following standard protocols, and fluorescent images (including EGFP) were captured using a Zeiss 510 confocal microscope and imported in Amira 2.2 to adjust their brightness and contrast and then imported in Photoshop 7.0 to assemble them in figures.

Samples for western blots were prepared by crushing third instar larvae in modified HL-3 with 0.4% Triton X-100 and proteinase inhibitors on ice and then boiling them in sample buffer for 5 min. Western blots were run and quantified according to standard protocols.

Antibodies and concentrations for immunohistochemistry/western blotting: α-adaptin (Gonzalez-Gaitan and Jackle, 1997) 1:500/1:5000; Dynamin (Upstate) 1:200/0.125 μg/ml; Eps15 (Koh et al., 2007) 1:5000/1:10000; Endophilin (Verstreken et al., 2002) 1:200/1:5000; Lap (AP180) (Zhang et al., 1998) 1:150/1:2500; Dap160 (Roos and Kelly, 1999) 1:500/1:5000; Stoned B (Phillips et al., 2000) 1:200/1:5000. Antibodies for immunohistochemistry: DLG (mouse; 4F3) (Parnas et al., 2001) 1:50; DLG (rabbit) (Kwang Choi, BCM) 1:500; HRP (Jackson Labs) 1:500; GluRIIA (mouse; 8B4) 1:50 (Schuster et al., 1991); and GLUR-III/IIC 1:500 (Marrus et al., 2004). Cy3 (Jackson ImmunoResearch) or Alexa 488 (Invitrogen) conjugated antibodies were used at 1:250. HRP-conjugated antibodies (Jackson ImmunoResearch) were used at 1:2500.

Labeling intensity of endocytic markers was quantified as described (Koh et al., 2004). Briefly, mutant and control samples were labeled together and imaged using identical settings. Pixel intensities inside the boutonic volumes, circumscribed by an independent marker, were calculated using Amira 2.2.

For quantification of endocytic markers we used DLG labeling as an independent outline of the boutonic volume and subtracted background labeling in the muscle.

For each lipid-GFP probe at least three controls and three mutant animals were labeled together with a synaptic marker (anti-HRP). GFP fluorescence of controls and mutants was imaged using identical settings, and using the synaptic marker as an outline of the synapse, we measured absolute GFP fluorescence intensity and normalized this to control values.

Electrophysiology and FM1-43 Dye Uptake and Live Imaging

ERGs and current clamp (CC) recordings were performed as described (Verstreken et al., 2002, 2003). Two electrode voltage clamp (TEVC) recordings were made in modified HL-3 ([in mM] NaCl 110; KCl 5; NaHCO$_3$ 10; HEPES 5; Sucrose 30; Trehalose 5; MgCl$_2$ 10; pH 7.2; CaCl$_2$ as indicated in the text; for minis, we added 5 μM TTX). Resting membrane potentials were between −55 and −65 mV and were clamped at −65 mV. Voltage errors were <1.5 mV for 100 nA EJCs, input resistances were ≥4 MΩ, and data were filtered at 1 kHz.

FM1-43 dye uptake experiments were performed as described in the text, and images were captured with a Zeiss MRm or on a Nikon Digital Sight DS2Mb-Wc camera using a 40× Zeiss or Nikon water immersion lens (NA 0.8) and analyzed and quantified as described (Verstreken et al., 2007).

Live imaging of PLCδ-PH-EGFP was performed as described in the Supplemental Experimental Procedures.

Transmission Electron Microscopy

TEM of PRs was performed as described in Hiesinger et al. (2005), and TEM of NMJ boutons was performed as described in Verstreken et al. (2003). Data were analyzed using Image-J.

SUPPLEMENTAL DATA

Supplemental Data include eight figures, Supplemental Experimental Procedures, and two tables and can be found with this article online at http://www.cell.com/neuron/supplemental/S0896-6273(09)00472-3.

REFERENCES

Achiriloaie, M., Barylko, B., and Albanesi, J.P. (1999). Essential role of the dynamin pleckstrin homology domain in receptor-mediated endocytosis. Mol. Cell. Biol. *19*, 1410–1415.

Babcock, M.C., Stowers, R.S., Leither, J., Goodman, C.S., and Pallanck, L.J. (2003). A genetic screen for synaptic transmission mutants mapping to the right arm of chromosome 3 in Drosophila. Genetics *165*, 171–183.

Bai, J., Tucker, W.C., and Chapman, E.R. (2004). PIP2 increases the speed of response of synaptotagmin and steers its membrane-penetration activity toward the plasma membrane. Nat. Struct. Mol. Biol. *11*, 36–44.

Bellen, H.J., Levis, R.W., Liao, G., He, Y., Carlson, J.W., Tsang, G., Evans-Holm, M., Hiesinger, P.R., Schulze, K.L., Rubin, G.M., et al. (2004). The BDGP gene disruption project: single transposon insertions associated with 40% of Drosophila genes. Genetics *167*, 761–781.

Betz, W.J., and Bewick, G.S. (1992). Optical analysis of synaptic vesicle recycling at the frog neuromuscular junction. Science *255*, 200–203.

Cao, Y.W., Jiang, C.L., and Jiang, T. (2006). Molecular cloning and preliminary analysis of a fragile site associated gene. Biomed. Environ. Sci. *19*, 392–398.

Chen, H., Fre, S., Slepnev, V.I., Capua, M.R., Takei, K., Butler, M.H., Di Fiore, P.P., and De Camilli, P. (1998). Epsin is an EH-domain-binding protein implicated in clathrin-mediated endocytosis. Nature *394*, 793–797.

Chintapalli, V.R., Wang, J., and Dow, J.A. (2007). Using FlyAtlas to identify better Drosophila melanogaster models of human disease. Nat. Genet. *39*, 715–720.

Cremona, O., Di Paolo, G., Wenk, M.R., Luthi, A., Kim, W.T., Takei, K., Daniell, L., Nemoto, Y., Shears, S.B., Flavell, R.A., et al. (1999). Essential role of phosphoinositide metabolism in synaptic vesicle recycling. Cell *99*, 179–188.

Daniels, R.W., Collins, C.A., Gelfand, M.V., Dant, J., Brooks, E.S., Krantz, D.E., and DiAntonio, A. (2004). Increased expression of the Drosophila vesicular glutamate transporter leads to excess glutamate release and a compensatory decrease in quantal content. J. Neurosci. *24*, 10466–10474.

Daniels, R.W., Collins, C.A., Chen, K., Gelfand, M.V., Featherstone, D.E., and DiAntonio, A. (2006). A single vesicular glutamate transporter is sufficient to fill a synaptic vesicle. Neuron *49*, 11–16.

Davis, G.W. (2006). Homeostatic control of neural activity: from phenomenology to molecular design. Annu. Rev. Neurosci. *29*, 307–323.

Davis, M.E., and Patrick, R.L. (1990). Diacylglycerol-induced stimulation of neurotransmitter release from rat brain striatal synaptosomes. J. Neurochem. *54*, 662–668.

Di Paolo, G., Pellegrini, L., Letinic, K., Cestra, G., Zoncu, R., Voronov, S., Chang, S., Guo, J., Wenk, M.R., and De Camilli, P. (2002). Recruitment and regulation of phosphatidylinositol phosphate kinase type 1 gamma by the FERM domain of talin. Nature *420*, 85–89.

Di Paolo, G., Moskowitz, H.S., Gipson, K., Wenk, M.R., Voronov, S., Obayashi, M., Flavell, R., Fitzsimonds, R.M., Ryan, T.A., and De Camilli, P. (2004). Impaired PtdIns(4,5)P2 synthesis in nerve terminals produces defects in synaptic vesicle trafficking. Nature *431*, 415–422.

Dietzl, G., Chen, D., Schnorrer, F., Su, K.C., Barinova, Y., Fellner, M., Gasser, B., Kinsey, K., Oppel, S., Scheiblauer, S., et al. (2007). A genome-wide transgenic RNAi library for conditional gene inactivation in Drosophila. Nature *448*, 151–156.

Fabian-Fine, R., Verstreken, P., Hiesinger, P.R., Horne, J.A., Kostyleva, R., Zhou, Y., Bellen, H.J., and Meinertzhagen, I.A. (2003). Endophilin promotes a late step in endocytosis at glial invaginations in Drosophila photoreceptor terminals. J. Neurosci. *23*, 10732–10744.

Fergestad, T., Davis, W.S., and Broadie, K. (1999). The stoned proteins regulate synaptic vesicle recycling in the presynaptic terminal. J. Neurosci. *19*, 5847–5860.

Ferguson, S.M., Brasnjo, G., Hayashi, M., Wolfel, M., Collesi, C., Giovedi, S., Raimondi, A., Gong, L.W., Ariel, P., Paradise, S., et al. (2007). A selective activity-dependent requirement for dynamin 1 in synaptic vesicle endocytosis. Science *316*, 570–574.

Gaidarov, I., Chen, Q., Falck, J.R., Reddy, K.K., and Keen, J.H. (1996). A functional phosphatidylinositol 3,4,5-trisphosphate/phosphoinositide binding domain in the clathrin adaptor AP-2 alpha subunit. Implications for the endocytic pathway. J. Biol. Chem. *271*, 20922–20929.

Gong, L.W., Di Paolo, G., Diaz, E., Cestra, G., Diaz, M.E., Lindau, M., De Camilli, P., and Toomre, D. (2005). Phosphatidylinositol phosphate kinase type I gamma regulates dynamics of large dense-core vesicle fusion. Proc. Natl. Acad. Sci. USA *102*, 5204–5209.

Gonzalez-Gaitan, M., and Jackle, H. (1997). Role of Drosophila alpha-adaptin in presynaptic vesicle recycling. Cell *88*, 767–776.

Golub, T., and Caroni, P. (2005). PI(4,5)P2-dependent microdomain assemblies capture microtubules to promote and control leading edge motility. J. Cell Biol. *169*, 151–165.

Harris, T.W., Hartwieg, E., Horvitz, H.R., and Jorgensen, E.M. (2000). Mutations in synaptojanin disrupt synaptic vesicle recycling. J. Cell Biol. *150*, 589–600.

Hassan, B.A., Prokopenko, S.N., Breuer, S., Zhang, B., Paululat, A., and Bellen, H.J. (1998). skittles, a Drosophila phosphatidylinositol 4-phosphate 5-kinase, is required for cell viability, germline development and bristle morphology, but not for neurotransmitter release. Genetics *150*, 1527–1537.

Haucke, V. (2003). Where proteins and lipids meet: membrane trafficking on the move. Dev. Cell *4*, 153–157.

Hiesinger, P.R., Fayyazuddin, A., Mehta, S.Q., Rosenmund, T., Schulze, K.L., Zhai, R.G., Verstreken, P., Cao, Y., Zhou, Y., Kunz, J., and Bellen, H.J. (2005). The v-ATPase V0 subunit a1 is required for a late step in synaptic vesicle exocytosis in *Drosophila*. Cell *121*, 607–620.

Horn, R. (2005). Electrifying phosphatases. Sci. STKE *2005*, pe50.

Jost, M., Simpson, F., Kavran, J.M., Lemmon, M.A., and Schmid, S.L. (1998). Phosphatidylinositol-4,5-bisphosphate is required for endocytic coated vesicle formation. Curr. Biol. *8*, 1399–1402.

Jung, N., and Haucke, V. (2007). Clathrin-mediated endocytosis at synapses. Traffic *8*, 1129–1136.

Kasprowicz, J., Kuenen, S., Miskiewicz, K., Habets, R.L., Smitz, L., and Verstreken, P. (2008). Inactivation of clathrin heavy chain inhibits synaptic recycling but allows bulk membrane uptake. J. Cell Biol. *182*, 1007–1016.

Koh, T.W., Verstreken, P., and Bellen, H.J. (2004). Dap160/intersectin acts as a stabilizing scaffold required for synaptic development and vesicle endocytosis. Neuron *43*, 193–205.

Koh, T.W., Korolchuk, V.I., Wairkar, Y.P., Jiao, W., Evergren, E., Pan, H., Zhou, Y., Venken, K.J., Shupliakov, O., Robinson, I.M., O'Kane, C.J., and Bellen, H.J. (2007). Eps15 and Dap160 control synaptic vesicle membrane retrieval and synapse development. J. Cell Biol. *178*, 309–322.

Kuo, M.T., Wei, Y., Yang, X., Tatebe, S., Liu, J., Troncoso, P., Sahin, A., Ro, J.Y., Hamilton, S.R., and Savaraj, N. (2006). Association of fragile site-associated (FSA) gene expression with epithelial differentiation and tumor development. Biochem. Biophys. Res. Commun. *340*, 887–893.

Lemmon, M.A. (2003). Phosphoinositide recognition domains. Traffic *4*, 201–213.

Majumdar, A., Ramagiri, S., and Rikhy, R. (2006). Drosophila homologue of Eps15 is essential for synaptic vesicle recycling. Exp. Cell Res. *312*, 2288–2298.

Manak, J.R., Dike, S., Sementchenko, V., Kapranov, P., Biemar, F., Long, J., Cheng, J., Bell, I., Ghosh, S., Piccolboni, A., and Gingeras, T.R. (2006). Biological function of unannotated transcription during the early development of Drosophila melanogaster. Nat. Genet. *38*, 1151–1158.

Mani, M., Lee, S.Y., Lucast, L., Cremona, O., Di Paolo, G., De Camilli, P., and Ryan, T.A. (2007). The dual phosphatase activity of synaptojanin1 is required for both efficient synaptic vesicle endocytosis and reavailability at nerve terminals. Neuron *56*, 1004–1018.

Marie, B., Sweeney, S.T., Poskanzer, K.E., Roos, J., Kelly, R.B., and Davis, G.W. (2004). Dap160/intersectin scaffolds the periactive zone to achieve high-fidelity endocytosis and normal synaptic growth. Neuron *43*, 207–219.

Marrus, S.B., Portman, S.L., Allen, M.J., Moffat, K.G., and DiAntonio, A. (2004). Differential localization of glutamate receptor subunits at the Drosophila neuromuscular junction. J. Neurosci. *24*, 1406–1415.

Martin, T.F. (1998). Phosphoinositide lipids as signaling molecules: common themes for signal transduction, cytoskeletal regulation, and membrane trafficking. Annu. Rev. Cell Dev. Biol. *14*, 231–264.

McKay, R.M., McKay, J.P., Avery, L., and Graff, J.M. (2003). C elegans: a model for exploring the genetics of fat storage. Dev. Cell *4*, 131–142.

Micheva, K.D., Holz, R.W., and Smith, S.J. (2001). Regulation of presynaptic phosphatidylinositol 4,5-biphosphate by neuronal activity. J. Cell Biol. *154*, 355–368.

Milosevic, I., Sorensen, J.B., Lang, T., Krauss, M., Nagy, G., Haucke, V., Jahn, R., and Neher, E. (2005). Plasmalemmal phosphatidylinositol-4,5-bisphosphate level regulates the releasable vesicle pool size in chromaffin cells. J. Neurosci. *25*, 2557–2565.

Newsome, T.P., Asling, B., and Dickson, B.J. (2000). Analysis of Drosophila photoreceptor axon guidance in eye-specific mosaics. Development *127*, 851–860.

Nonet, M.L., Holgado, A.M., Brewer, F., Serpe, C.J., Norbeck, B.A., Holleran, J., Wei, L., Hartwieg, E., Jorgensen, E.M., and Alfonso, A. (1999). UNC-11, a Caenorhabditis elegans AP180 homologue, regulates the size and protein composition of synaptic vesicles. Mol. Biol. Cell *10*, 2343–2360.

Parks, A.L., Cook, K.R., Belvin, M., Dompe, N.A., Fawcett, R., Huppert, K., Tan, L.R., Winter, C.G., Bogart, K.P., Deal, J.E., et al. (2004). Systematic generation of high-resolution deletion coverage of the Drosophila melanogaster genome. Nat. Genet. *36*, 288–292.

Parnas, D., Haghighi, A.P., Fetter, R.D., Kim, S.W., and Goodman, C.S. (2001). Regulation of postsynaptic structure and protein localization by the Rho-type guanine nucleotide exchange factor dPix. Neuron *32*, 415–424.

Phillips, A.M., Smith, M., Ramaswami, M., and Kelly, L.E. (2000). The products of the Drosophila stoned locus interact with synaptic vesicles via synaptotagmin. J. Neurosci. *20*, 8254–8261.

Poskanzer, K.E., Marek, K.W., Sweeney, S.T., and Davis, G.W. (2003). Synaptotagmin I is necessary for compensatory synaptic vesicle endocytosis in vivo. Nature *426*, 559–563.

Ramaswami, M., Krishnan, K.S., and Kelly, R.B. (1994). Intermediates in synaptic vesicle recycling revealed by optical imaging of *Drosophila* neuromuscular junctions. Neuron *13*, 363–375.

Rhee, J.S., Betz, A., Pyott, S., Reim, K., Varoqueaux, F., Augustin, I., Hesse, D., Sudhof, T.C., Takahashi, M., Rosenmund, C., and Brose, N. (2002). Beta phorbol ester- and diacylglycerol-induced augmentation of transmitter release is mediated by Munc13s and not by PKCs. Cell *108*, 121–133.

Roos, J., and Kelly, R.B. (1999). The endocytic machinery in nerve terminals surrounds sites of exocytosis. Curr. Biol. *9*, 1411–1414.

Schiavo, G., Gu, Q.M., Prestwich, G.D., Sollner, T.H., and Rothman, J.E. (1996). Calcium-dependent switching of the specificity of phosphoinositide binding to synaptotagmin. Proc. Natl. Acad. Sci. USA *93*, 13327–13332.

Schuske, K.R., Richmond, J.E., Matthies, D.S., Davis, W.S., Runz, S., Rube, D.A., van der Bliek, A.M., and Jorgensen, E.M. (2003). Endophilin is required for synaptic vesicle endocytosis by localizing synaptojanin. Neuron *40*, 749–762.

Schuster, C.M., Ultsch, A., Schloss, P., Cox, J.A., Schmitt, B., and Betz, H. (1991). Molecular cloning of an invertebrate glutamate receptor subunit expressed in Drosophila muscle. Science *254*, 112–114.

Sladeczek, F. (1987). Putative role of inositol phospholipid metabolism in neurons. Biochimie *69*, 287–296.

Stahelin, R.V., Long, F., Peter, B.J., Murray, D., De Camilli, P., McMahon, H.T., and Cho, W. (2003). Contrasting membrane interaction mechanisms of AP180 N-terminal homology (ANTH) and epsin N-terminal homology (ENTH) domains. J. Biol. Chem. *278*, 28993–28999.

Stimson, D.T., Estes, P.S., Rao, S., Krishnan, K.S., Kelly, L.E., and Ramaswami, M. (2001). Drosophila stoned proteins regulate the rate and fidelity of synaptic vesicle internalization. J. Neurosci. *21*, 3034–3044.

Stowers, R.S., and Schwarz, T.L. (1999). A genetic method for generating Drosophila eyes composed exclusively of mitotic clones of a single genotype. Genetics *152*, 1631–1639.

van der Bliek, A.M., and Meyerowitz, E.M. (1991). Dynamin-like protein encoded by the Drosophila shibire gene associated with vesicular traffic. Nature *351*, 411–414.

Van Epps, H.A., Hayashi, M., Lucast, L., Stearns, G.W., Hurley, J.B., De Camilli, P., and Brockerhoff, S.E. (2004). The zebrafish nrc mutant reveals a role for the polyphosphoinositide phosphatase synaptojanin 1 in cone photoreceptor ribbon anchoring. J. Neurosci. *24*, 8641–8650.

Varnai, P., and Balla, T. (1998). Visualization of phosphoinositides that bind pleckstrin homology domains: calcium- and agonist-induced dynamic changes and relationship to myo-[3H]inositol-labeled phosphoinositide pools. J. Cell Biol. *143*, 501–510.

Varnai, P., and Balla, T. (2006). Live cell imaging of phosphoinositide dynamics with fluorescent protein domains. Biochim. Biophys. Acta *1761*, 957–967.

Venken, K.J., He, Y., Hoskins, R.A., and Bellen, H.J. (2006). P[acman]: a BAC transgenic platform for targeted insertion of large DNA fragments in D. melanogaster. Science *314*, 1747–1751.

Verstreken, P., Kjaerulff, O., Lloyd, T.E., Atkinson, R., Zhou, Y., Meinertzhagen, I.A., and Bellen, H.J. (2002). Endophilin mutations block clathrin-mediated endocytosis but not neurotransmitter release. Cell *109*, 101–112.

Verstreken, P., Koh, T.W., Schulze, K.L., Zhai, R.G., Hiesinger, P.R., Zhou, Y., Mehta, S.Q., Cao, Y., Roos, J., and Bellen, H.J. (2003). Synaptojanin is recruited by endophilin to promote synaptic vesicle uncoating. Neuron *40*, 733–748.

Verstreken, P., Ohyama, T., and Bellen, H.J. (2007). FM 1–43 labeling at the Drosophila neuromuscular junction. Methods Mol. Biol. *440*, 349–369.

Vicinanza, M., D'Angelo, G., Di Campli, A., and De Matteis, M.A. (2008). Function and dysfunction of the PI system in membrane trafficking. EMBO J. *27*, 2457–2470.

Voronov, S.V., Frere, S.G., Giovedi, S., Pollina, E.A., Borel, C., Zhang, H., Schmidt, C., Akeson, E.C., Wenk, M.R., Cimasoni, L., et al. (2008). Synaptojanin 1-linked phosphoinositide dyshomeostasis and cognitive deficits in mouse models of Down's syndrome. Proc. Natl. Acad. Sci. USA *105*, 9415–9420.

Wenk, M.R., and De Camilli, P. (2004). Protein-lipid interactions and phosphoinositide metabolism in membrane traffic: insights from vesicle recycling in nerve terminals. Proc. Natl. Acad. Sci. USA *101*, 8262–8269.

Wucherpfennig, T., Wilsch-Brauninger, M., and Gonzalez-Gaitan, M. (2003). Role of Drosophila Rab5 during endosomal trafficking at the synapse and evoked neurotransmitter release. J. Cell Biol. *161*, 609–624.

York, J.D. (2006). Regulation of nuclear processes by inositol polyphosphates. Biochim. Biophys. Acta *1761*, 552–559.

Zhai, R.G., Hiesinger, P.R., Koh, T.W., Verstreken, P., Schulze, K.L., Cao, Y., Jafar-Nejad, H., Norga, K.K., Pan, H., Bayat, V., et al. (2003). Mapping Drosophila mutations with molecularly defined P element insertions. Proc. Natl. Acad. Sci. USA *100*, 10860–10865.

Zhang, B., Koh, Y.H., Beckstead, R.B., Budnik, V., Ganetzky, B., and Bellen, H.J. (1998). Synaptic vesicle size and number are regulated by a clathrin adaptor protein required for endocytosis. Neuron *21*, 1465–1475.

Zoncu, R., Perera, R.M., Sebastian, R., Nakatsu, F., Chen, H., Balla, T., Ayala, G., Toomre, D., and De Camilli, P.V. (2007). Loss of endocytic clathrin-coated pits upon acute depletion of phosphatidylinositol 4,5-bisphosphate. Proc. Natl. Acad. Sci. USA *104*, 3793–3798.